Dynamic cell culturing and its application to micropatterned, elastin-like protein-modified poly(*N*-isopropylacrylamide) scaffolds

Nihan Ozturk [a], Alessandra Girotti [b,d], Gamze T. Kose [c], José C. Rodríguez-Cabello [b,d], Vasif Hasirci [a,*]

[a] *METU, BIOMAT, Department of Biological Sciences, Biotechnology Research Unit, Inonu Bulvari, Ankara 06531, Turkey*
[b] *GIR BIOFORGE (Universidad de Valladolid) Pº de Belén s/n 47011 Valladolid, Spain*
[c] *Yeditepe University, Department of Genetics and Bioengineering, 34755 Istanbul, Turkey*
[d] *CIBER-BBN Networking Centre on Bioengineering, Biomaterials, and Nanomedicine, Valladolid, Spain*

a r t i c l e i n f o

Keywords:
Thermoresponsive
pNIPAM
Mechanical stress
Elastin-like protein
Bone tissue engineering

a b s t r a c t

In this study a tissue engineering scaffold was constructed from poly(*N*-isopropylacrylamide) (pNIPAM) to study the influence of strain on cell proliferation and differentiation. The effect of surface chemistry and topography on bone marrow mesenchymal stem cells was also investigated. Micropatterned pNIPAM films (channels with 10 μm groove width, 2 μm ridge width, 20 μm depth) were prepared by photopolymerization. The films were chemically modified by adsorption of a genetically engineered and temperature sensitive elastin-like protein (ELP). Dynamic conditions were generated by repeated temperature changes between 29 °C and 37 °C. ELP presence on the films enhanced initial cell attachment two fold (Day 1 cell number on films with ELP and without ELP were 27.6×10^4 and 13.2×10^4, respectively) but had no effect on proliferation in the long run. ELP was crucial for maintaining the cells attached on the surface in dynamic culturing (Day 7 cell numbers on the films with and without ELP were 81.4×10^4 and 12.1×10^4, respectively) and this enhanced the ability of pNIPAM films to transfer mechanical stress on the cells. Dynamic conditions improved cell proliferation (Day 21 cell numbers with dynamic and with static groups were 180.4×10^4 and 157.7×10^4, respectively) but decreased differentiation (Day 14 specific ALP values on the films of static and dynamic groups were 6.6 and 3.5 nmol/min/cell, respectively). Thus, a physically and chemically modified pNIPAM scaffold had a positive influence on the population of the scaffolds under dynamic culture conditions.

1. Introduction

The loss of bone because of trauma, cancer, osteoporosis or congenital abnormalities is a serious clinical problem. The most common methods employed in the repair of these defects are the use of autologous grafts or alloplastic nonbiological implants [1,2]. Autologous tissue grafting is the prevalent option in most cases but has constraints such as the availability of donor tissue, morbidity at the donor site, and time-consuming surgery.

Tissue engineering, as an alternative approach, seems to be promising as it aims to create fully functional and biocompatible "living" grafts in desired quantity and dimension that have the potential to integrate with the surrounding native tissue eliminating the problems of donor scarcity, immune rejection and supply limitation [3,4].

Scaffold is the most essential component of tissue engineering. All biological, physical and chemical parameters that affect cell function and tissue morphogenesis have to be taken into account when designing a scaffold [5]. Especially important are surface topography, and chemical and biological entities that improve cell–material interaction.

Since cell attachment is the first major step for the later cell behaviors, surface modification by attaching cell adhesive molecules is widely used. Many extracellular matrix (ECM) components such as collagen and fibronectin contain sequences such as arginine-glycine-aspartic acid (RGD) specific for cell attachment. Although natural ECM proteins show excellent cell attachment, they still have drawbacks because the control of their chemical and physical properties is limited and their conformation and composition is different after reconstitution [6]. Genetic engineering has enabled the control of production and addition of new features to polypeptides which make them more useful in tissue engineering studies. They can be produced in large amounts using microbial technology. Modification of sequence, chain length, topography and stereochemistry of the polypeptides make the

control of their physical and mechanical properties such as transition temperature, stiffness and hardness possible. They can be further functionalized to exhibit responsiveness to pH, light and other stimuli, such as electrochemical potential or concentration. ELPs are among these genetically engineered biopolymers consisting of oligomeric repeats of the pentapeptide sequence VPGXG, where X is any amino acid except proline, derived from a native sequence found in the structural protein elastin. In aqueous solutions below a critical transition temperature (T_t) these polypeptide chains are soluble in the form of disordered, random coils. Above the T_t, the polymer chains adopt a dynamic, regular, non-random structure and their solubility is lowered [7–10]. They are widely used in many fields of biotechnology and biomedicine including bioseparation [11], drug delivery [12,13] and tissue engineering [14,15].

Most of the cells in the body are subjected to mechanical stimuli originating from a wide variety of sources which they need for proper functioning. Bone grows in a highly dynamic environment, experiencing compressive and tensile as well as shear stress (the last one as a result of enhanced fluid flow in the canalicular network caused by mechanical loading) [16]. Tissues respond to them through a cascade of signal transduction steps resulting in the regulation of cell functions like cytoskeleton organization, gene expression, protein synthesis, proliferation, differentiation and apoptosis. A typical problem, bone density decrease, is observed when the skeleton is not loaded enough, i.e. due to the microgravity in space flights [17] and during bed-rest [18]. Therefore, exercise regimes have been introduced to maintain bone mass and to accelerate bone mass recovery in space or after bed rest [19]. In order to study the effect of mechanical stimuli on bone cells, several different approaches such as fluid flow [20,21], stretching and fluid flow using four point bending [22], hydrodynamic pressure [23], stretching and compression [24] are employed.

In this study, the goal was to modify the surface topography and chemistry of a non-degradable thermosensitive 2D scaffold and applying temperature changes rhythmically to flex and contract the scaffold to apply mechanical stress to the cells. The dynamic culturing was expected to improve bone formation. A micropatterned film carrying cell adhesion amino acid sequences was prepared. For the first time in the literature, thermal responsiveness was used to apply mechanical stress on cells under *in vitro* conditions. To achieve these, a thermoresponsive polymer, poly(*N*-isopropylacrylamide) (pNIPAM), was utilized as the scaffold material. pNIPAM, becomes hydrophilic and dissolves below 32 °C [25]. Crosslinked pNIPAM films would swell and shrink upon temperature change and this would apply mechanical stress on the cells seeded onto them. Thermoresponsive and cell adhesive (RGD containing) ELP was adsorbed on the pNIPAM films to improve cell attachment and a better cell–material communication.

2. Materials and methods

2.1. Materials

N-Isopropylacrylamide (NIPAM), cacodylic acid (sodium salt), amphotericin B, penicillin–streptomycin, trypsin–EDTA (0.25%), β-glycerophosphate, dexamethasone, FITC-labelled phalloidin and 4′,6-diamidino-2-phenylindole dihydrochloride (DAPI) were purchased from Sigma–Aldrich Co. (USA). Elastin-like polypeptide containing RGD amino acid sequences (complete amino acid sequence is MESLLP[[(VPGIG)$_2$(VPGKG)(VPGIG)$_2$]$_2$AVTGRGDSPASS[(VPGIG)$_2$(VPGKG)(VPGIG)$_2$]$_2$]$_8$V) was produced and isolated from *Escherichia coli* (*E. coli*) at the University of Valladolid (Spain). Synthetic oligonucleotides were purchased from IBA GmbH (Goettinhem, Germany), *Taq* DNA polymerase and the restriction enzyme Eam 1104 I from Stratagene. DNA ligase, Shrimp Alkaline Phosphatase (S.A.P) and Antartic alkaline phosphatase from NewEngland Biolabs. PCR amplifications were performed in an Eppendorf AG 22331 termocycler. Gel photographs were taken with Gel logic 100 Imaging System and the Kodak 3.6 software. *E. coli* strain BLR(DE3) was obtained from Novagen (Madison) ampicillin and isopropyl-1-β-D-thiogalactoside (IPTG) from Apollo Scientific (Bredbury, UK).

Tetracycline was a gift of Dr. I. Yılmaz of FAKO Ilac. San. (Istanbul, Turkey). Fetal calf serum (FCS) and Dulbecco's Modified Eagle's Medium (DMEM; high glucose) were purchased from Gibco (USA). Colorless DMEM (without sodium pyruvate and phenol red) was purchased from HyClone® (USA). Alamar Blue was from Biosource (USA). Alkaline Phosphatase 307 Kit was purchased from Randox® (UK). NucleoCounter reagents and nucleocasettes were purchased from Chemometec (Denmark).

2.2. Protein expression and purification

Standard genetic engineering techniques were performed to construct ELP gene. The polymer biosynthesis was carried out using *E. coli* system of recombinant protein production, while its purification was performed with several cycles of temperature-depending reversible precipitations as described elsewhere [13]. Purified ELP was dialyzed in cold type I water and then lyophilized.

The purity and molecular weight of recombinant ELP were verified by sodium dodecyl sulphate polyacrylamide gel electrophoresis (SDS-PAGE), and mass spectroscopy (MALDI-TOF/MS), whereas; the correctness of sequence was checked by amino acid composition analysis and amino acid sequencing.

2.3. Synthesis and preparation of pNIPAM films

Poly(*N*-isopropylacrylamide) (pNIPAM) was synthesized by photopolymerization using EGDMA as the crosslinker and AIBN as the photoinitiator. AIBN (0.3 mol% w.r.t. NIPAM), NIPAM (50% w/v) and EGDMA (2.4 mol% w.r.t NIPAM) were dissolved in isopropanol/water (1:1) and exposed to UV for 6 h in a Petri dish. The polymer was washed with distilled water and dried.

Patterned pNIPAM films were produced by placing silicon templates produced by photolithography (groove width: 2 μm, ridge width: 10 μm, depth: 20 μm, wall angle: 54.7°) facing upward at the bottom of the Petri dishes before introducing the polymerization solution.

2.4. Characterization of films

2.4.1. Swelling of pNIPAM films with temperature

Water uptake by the polymer discs at various temperatures was studied by gravimetry in the range 20–37 °C. At each temperature, pNIPAM samples were immersed in distilled water for 24 h, mopped slightly with moistened filter, and weighed.

2.4.2. Water contact angle

Unpatterned pNIPAM films (ca. 1 cm in diameter) were maintained at 29 °C and 37 °C for 48 h in distilled water. The excess water on the surface of the films was removed by gently touching tissue paper to the surface. Water contact angle measurements were performed using a goniometer (CAM 200, KSV Ltd, Finland) using at least 6 droplets.

2.5. In vitro studies

2.5.1. Isolation of bone marrow mesenchymal stem cells (BMSC)

BMSC were isolated from 6 week old male Sprague–Dawley rats as described elsewhere [26]. Briefly, the rats were euthanized by diethyl ether inhalation and disinfected with 1:1 (v/v) betadine/70% EtOH. Surgery took place in the laminar flow hood under aseptic conditions. The femurs and tibia of the rats were excised, washed in DMEM with 1000 U/mL penicillin and 1000 mg/mL streptomycin and the bone marrow was flushed out with primary medium (DMEM containing 10% FCS, 100 U/mL penicillin and 100 μg/mL streptomycin), centrifuged (5 min, 3000 rpm) (RotaFix 32, Hettich Zentrifugen, Germany), resuspended in primary medium, and plated in T-75 flasks (cells from one femur per flask). Primary cultures were incubated in a CO_2 incubator (Sanyo MCO-17 AIC, Japan) at 37 °C and 5% CO_2 and left undisturbed for 2 days to enable cell attachment. The medium was then discarded and the cells were washed with phosphate buffered saline (PBS) (10 mM, pH 7.4). The medium was refreshed every two days. Primary cells were cryopreserved in FCS containing 10% DMSO until use.

2.5.2. Surface modification with ELP adsorption

pNIPAM films were cut in 1 cm^2 pieces and UV sterilized for 30 min on each side. ELP solution was filtered through 0.2 μ pore sized syringe filters (Orange Scientific) and then, top surfaces of the films were modified by adsorption of ELP (0.1% w/v). Control group was unmodified.

2.5.3. Cell seeding and static culture on films

First passage BMSC grown in primary medium were detached from the tissue culture flasks by using 0.05% trypsin for 5 min at 37 °C, then centrifuged for 5 min at 3000 rpm, and resuspended in high glucose DMEM supplemented with 10% FCS, 100 U/mL penicillin, and 100 μg/mL streptomycin. Cell number was determined using NucleoCounter (ChemoMetec A/S, Denmark). Dry films were placed in sterile

24-well plates (Orange Scientific) and 2×10^5 cells suspended in 30 mL were seeded on them and kept undisturbed for 3 h in the CO_2 incubator (5% CO_2) at 37 °C. Then, 1 mL of complete medium (high glucose DMEM supplemented with 100 units/mL penicillin, 100 mg/mL streptomycin, 4% amphotericin B, 10% FCS, 10 mM b-glycerophosphate, 50 mg/mL L-ascorbic acid and 10 nM dexamethasone) was added on the films to promote osteogenic differentiation of the BMSC. Tissue culture polystyrene (TCPS) served as the positive control.

2.5.4. Dynamic culture of the BMSC

Mechanical stress on the cells was generated by changing the temperature between 37 °C to 29 °C to shrink and stretch the pNIPAM films. The 24-well tissue culture plates carrying the cell seeded pNIPAM films were taken out of the CO_2 incubator at 37 °C, placed in the laminar flow hood and the caps of the plates were opened for 5 min to achieve rapid temperature change. Then the caps were replaced and the flasks were transferred to another CO_2 incubator maintained at 29 °C (5% CO_2) (Heal force HF90, Shangai Lishen Scientific Equipment Co., Ltd., China). After incubating at 29 °C for 10 min, the plates were again transferred to the previous CO_2 incubator (37 °C). Ten cycles of temperature switches were applied for 5 days starting on the second day post cell seeding.

2.5.5. Cell proliferation

Alamar Blue assay was performed to determine cell proliferation on Days 1, 7, 14 and 21 of culture. The cell seeded and control (cell-free) films were transferred to fresh wells and washed with PBS. Alamar Blue solution (1 mL, 10% in colorless DMEM medium) was added into each well and the cells were incubated for 1 h with Alamar Blue solution in a CO_2 incubator at 37 °C. Then, 200 mL of the Alamar Blue solution from each well was added into a 96-well tissue culture plate in triplicate and their absorbances were measured at 595 nm and 570 nm with the Elisa Plate Reader (Maxline Vmax®, Molecular Devices, USA). Viable cell numbers were determined using a calibration curve.

2.5.6. Determination of ALP activity

ALP assay was performed for cell seeded and control (cell-free) films and TCPS cultured for 7, 14 and 21 days. Medium in the wells were removed, the films were washed with PBS and transferred into 0.5 mL Tris buffer (10 mM, pH 7.5, 0.1% Triton® X-100) for cell lysis and stored at -20 °C. The samples were freeze-thawed (-20 to 37 °C) three times to ensure complete lysis, sonicated for 5 min at 25 W (Ultrasonic Homogenizer, Cole Parmer, USA) on ice with 30 s on, 30 s off cycles, and centrifuged (2000 rpm, 10 min). 10 mL of each supernatant was added to 240 mL of substrate (*p*-nitrophenyl phosphate reconstituted with $MgCl_2$–diethanolamine buffer supplied by Randox AP307 kit). The time dependent absorbance of the mixture was obtained at 405 nm every min for a total of twelve min by the Elisa Plate Reader (readings were performed in duplicate). The data was analyzed by using the slope of the calibration curve previously prepared with *p*-nitrophenol as the substrate. Specific ALP activity (ALP activity/cell) was calculated as ALP activity per sample per cell.

2.5.7. Fluorescence microscopy

Cells on the films were observed by fluorescence microscopy (Leica, DFC 300 FX, Germany) on Day 21 of the culture. After fixation with 4% formaldehyde (in 0.01 M PBS, pH 7.4) for 30 min, the films were washed in PBS, the cell membranes were permeabilized with 1% Triton X-100 (in 0.01 M PBS) for 5 min and washed in PBS before the film surfaces were blocked with 1% BSA solution for 30 min at 37 °C. Then they were washed again in PBS and stained with 1 mg/mL FITC-labelled Phalloidin (Sigma–Aldrich Co., USA) in 0.1% PBS–BSA solution for 5 min at 37 °C. The films were washed in 1% PBS–BSA solution and they were double stained with the nuclear stain DAPI (Sigma–Aldrich Co., USA) at a concentration of 1 mg/mL in 0.1% PBS–BSA solution for 5 min at 37 °C after Phalloidin. The films were again washed in 1% PBS–BSA solution and examined by fluorescence microscopy with the filter for excitation at 488 nm for FITC-labelled Phalloidin and UV filter for DAPI.

2.5.8. Scanning electron microscopy (SEM)

On Days 7, 14 and 21 of culture, cells were fixed with glutaraldehyde (2.5% in 0.1 M, pH 7.4 sodium cacodylate buffer) for 2 h. After fixation, they were washed three times with cacodylate buffer with 30 min incubation periods, the samples were frozen at -80 °C over night, and freeze dried. The dry samples were gold coated under vacuum and then examined by a Scanning Electron Microscope (SEM) (FEI QUANTA 400-F, Holland) at the METU Central Laboratory. The surfaces of these samples were also scanned via X-ray photoelectron spectroscopy (XPS) and calcium (Ca) and phosphate (P) contents were determined for Day 21 of culture.

2.5.9. Mineralization

In order to study the mineralization on the films, a differentiation medium containing 10 mg/mL tetracycline instead of other antibiotics (100 units/mL penicillin and 100 mg/mL streptomycin) was introduced to cells beginning on the 3rd day. On Day 21 of culture, the cells were washed with PBS (10 mM, pH 7.4), with 70% ethanol and fixed in 96% ethanol at 37 °C for 6 h [27]. The films were dried, and mineralization was studied using a fluorescence microscope (Leica, DFC 300 FX, Germany) at 480 nm.

2.6. Statistical analysis

The statistical analysis of the data was done by Student's *T*-test.

3. Results

3.1. Protein expression and purification

In order to verify the effectiveness of production and purification methods, SDS-PAGE, MALDI-TOF mass spectroscopy, and amino acid analysis were performed. SDS-PAGE electrophoresis (Fig. 1) of purified ELP sample confirmed its purity and

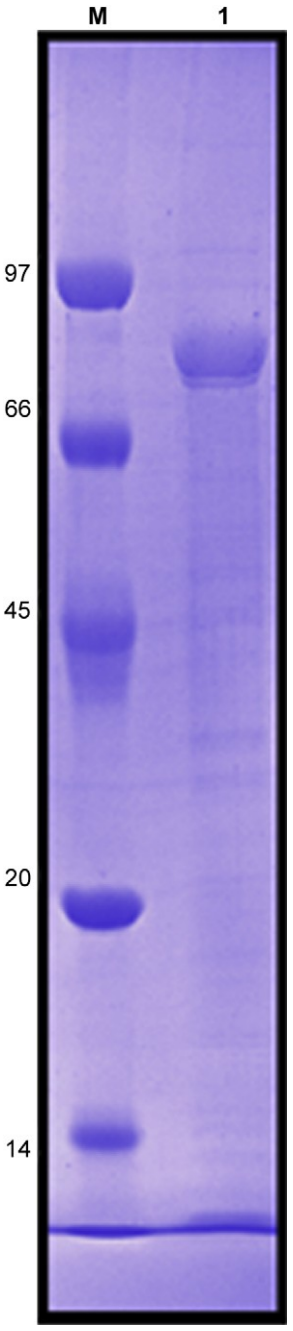

Fig. 1. Analysis of ELP purity by SDS-polyacrilamide gel electrophoresis. Lane M: Molecular standards, Lane 1: Purified polymer. Numbers on the left indicate the corresponding apparent MW values of the standard (in kDa).

monodisperse nature. Production yield of purified ELP was about 50 mg/L of bacterial culture. Fig. 2 shows the ELP MALDI-TOF mass spectrum, experimental molecular weight found by this technique matches well the expected molecular weight of the polymer (77733 Da) within the experimental error. The measured amino acid content fits with the theoretical composition (Table 1).

3.2. *Characterization of the films*

3.2.1. *Swelling*

Temperature responsiveness was studied gravimetrically in the range 20–37 °C (Fig. 3). The water content (WC) of polymer discs at different temperatures was calculated as WC ¼ ðWs – Wd=ÞWd, where W_s and W_d are the weights of wet and dry films, respectively.

A transition was observed between 25 and 33 °C, within which lies the LCST (w32 °C) of pNIPAM (Fig. 3). Swelling increased especially below 31 °C. The water content of the pNIPAM at 25 °C was almost 6 times that at 31 °C. In order not to damage the cells by exposure to low temperatures, the temperatures used in the dynamic incubation studies were selected as 29 °C and 37 °C, where there is a WC ratio of 3.5.

3.2.2. *Water contact angles*

After an incubation in water for 48 h at 29 °C and 37 °C, water contact angles of unpatterned pNIPAM films were measured as 60.5° ± 5.3 at 37 °C and 21.0° ± 5.7 at 29 °C. This finding indicates a significant increase in hydrophilicity upon temperature decrease, and explains the difference in swelling at these temperatures (Fig. 3).

Table 1
Theoretical and measured amino acid compositions of ELP.

Amino acid	Theoretical	Measured
Asp	8	8.17
Ser	25	26.93
Glu	1	1.50
Gly	336	356.3
Ala	16	15.23
Val	169	168.46
Met	1	2.34
Ile	128	118.05
Leu	2	4.61
Thr	8	6.73
Lys	32	29.01
Arg	8	9.46
Pro	169	168.46

3.2.3. *Calculation of strain applied to BMSC under dynamic conditions*

pNIPAM films were prepared eventually to use as cell carriers with a capacity to expand (swell) and contract with temperature and thus generating a stress on the BMSC seeded on the films. Strain of the films was calculated as:

$$e \;¼\; \frac{DL}{L_0} \;¼\; \frac{|L - L_0|}{L_0}$$

where; e is the strain, L_0 and L are the original and current length of the film. The strain upon variation of the temperature between 29 °C and 37 °C was calculated as 0.059 ± 0.023 (or roughly 6%)

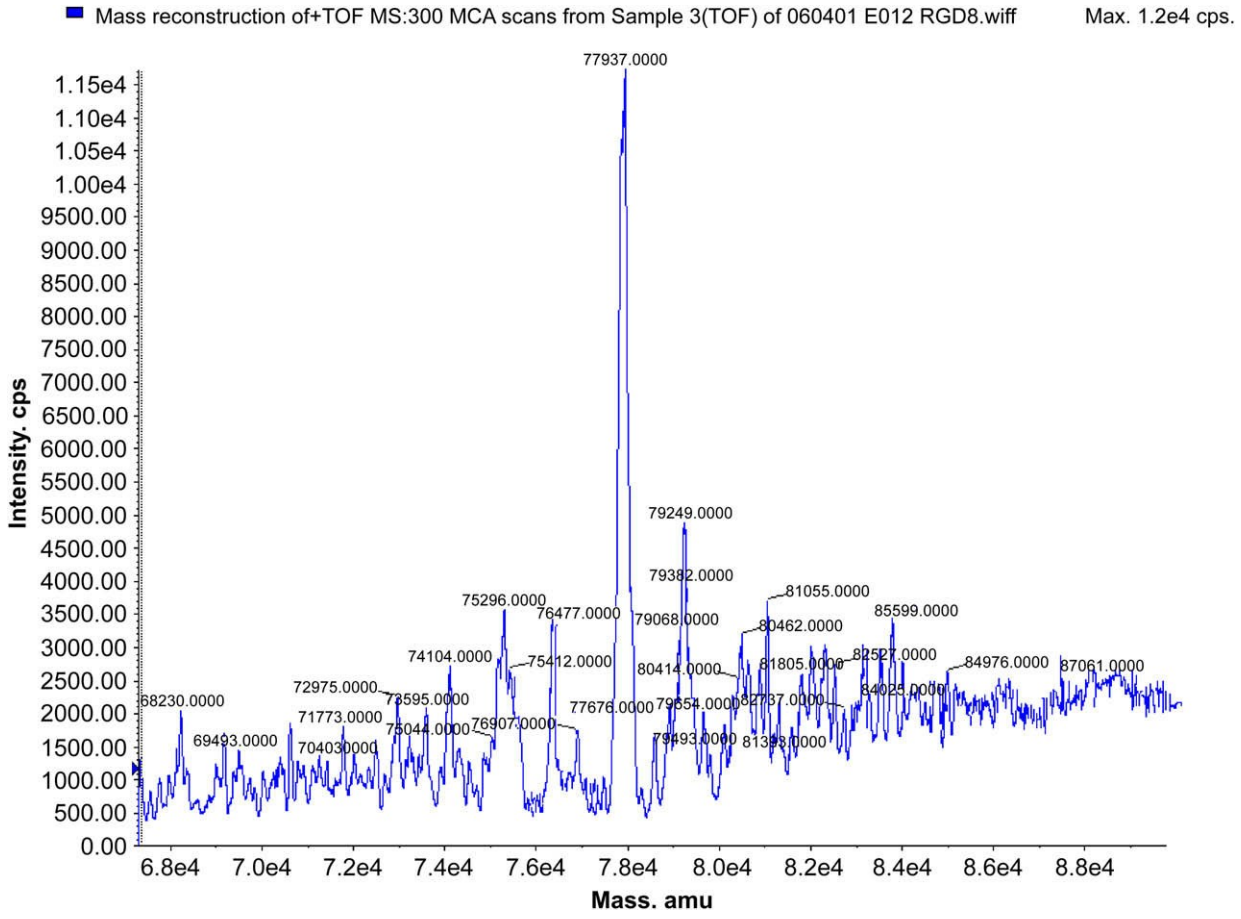

Fig. 2. Mass spectra (MALDI-TOF/MS) of ELP. The expected mass of the polypeptide is 77733 Da.

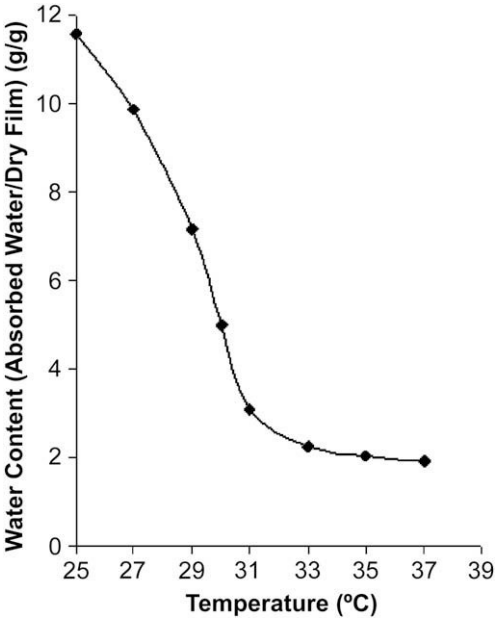

Fig. 3. Swelling of pNIPAM with temperature.

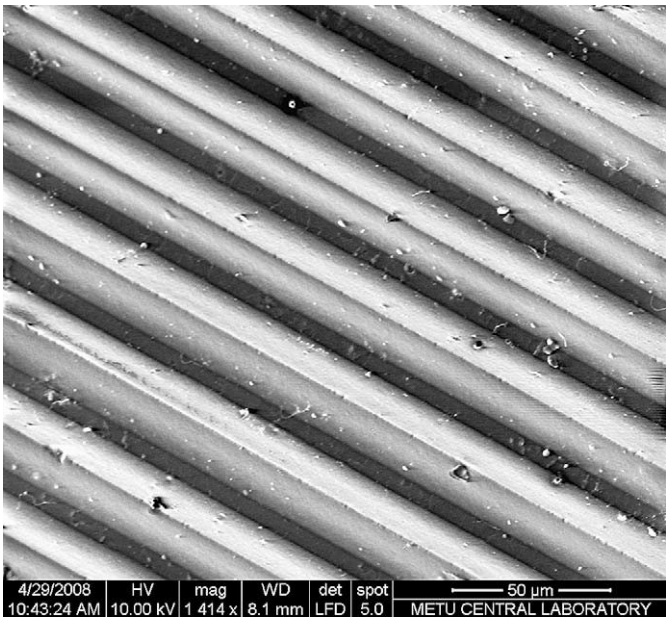

Fig. 4. SEM image of a patterned pNIPAM film (x1414).

(n ¼ 3). The large standard deviation might be the result of insufficient control of temperature in the laminar hood.

Strain is a dimensionless unit. 1 Strain is defined by some authors as 100% elongation [28]. 0.1% strain, is therefore, equal to 1000 mstrain and is in the physiological range in loaded bone tissue. Strain magnitudes between 1000 and 10,000 mstrain were reported to occur in the fracture site of a healing bone [28]. In comparison to these strain values, the mechanical strain generated by pNIPAM films under the conditions of this study was 6–60 fold higher.

3.2.4. SEM

SEM micrographs of cell seeding surfaces of patterned films presented in Fig. 4 show that the pattern could be transferred with high fidelity onto the pNIPAM films.

3.3. In vitro studies

3.3.1. Cell proliferation

Cell numbers were determined on Days 1, 7, 14 and 21 of culture on the samples of TCPS, unpatterned and patterned pNIPAM films with and without adsorbed ELP, cultured under static or dynamic conditions (Fig. 5).

First day results are indicative of cell adhesion and showed that the numbers of cells were generally higher on ELP adsorbed films and on TCPS than their ELP-free counterparts. This was expected because the ELP used in this experiment was designed to include the cell adhesive RGD amino acid sequences. This result also demonstrated that the adsorption process of ELP on films was successful.

One week results showed that the cell numbers on ELP adsorbed films were still higher than those on the films without ELP. As time progressed, the difference due to ELP presence disappeared. Dynamic conditions were observed to lead to decreased cell numbers when ELP was absent and increased cell numbers when it was present. The low cell number values obtained from the dynamic group without ELP were probably the result of weakened cell attachment especially at 29 °C where the hydrophilicity of pNIPAM is higher (see Section 3.2.2.). On the other hand, at 37 °C, which is above the LCST, cells can attach and proliferate on pNIPAM. Once more the effect of ELP on cell attachment was observed and it can be stated that the cells cultured under dynamic conditions retain themselves in attached form on the surface if ELP is present.

The cells on the films without ELP eventually reached comparable cell number values with those with ELP as well as the cells on the films cultured under static conditions. However, the cell number on Dy TCPS was lower than St TCPS at the end of the first week although the first day cell number was somewhat higher and the decrease in cell number continued through the third week. So this finding shows that the mechanical stress created under the dynamic conditions enhanced proliferation of cells on the films and compensated for the adverse effect of cyclic temperature change, whereas cyclic temperature change could not induce a stress on the TCPS and those cells were subject to the unfavorable temperatures (29 °C) of this process without benefiting from the positive effect of the dynamic incubation.

3.3.2. ALP activity

ALP activity was determined on the 7th, 14th and 21st days of culture. In the first week with the static group, the ALP activities were found to be low and they reached a maximum for all the samples on Day 14 (Fig. 6a) before decreasing again by Day 21. On Day 7 the highest ALP activity was obtained for St TCPS. ALP activities on films were found to increase dramatically on Day 14 with the lowest value obtained for St TCPS.

Day 7 ALP results obtained from dynamic group were generally lower than the static group (Fig. 6b). The ALP activity on Dy TCPS was the highest on Day 7 compared to the films cultured under dynamic conditions, but decreased by time. On Day 14, the ALP activity on the films increased dramatically as observed in the static group. Dy P reached the maximum value for ALP on Day 21, while for all the other films that were under dynamic and static conditions, the maximum values were detected on Day 14.

On the whole the activities under static conditions were higher than those under dynamic conditions regardless of the presence or absence of ELP.

Specific activities are the activities per cell. The specific ALP activities on Day 7 were lower than those on Day 14 in static and dynamic groups with the only exception of Dy TCPS, which followed a decreasing ALP activity trend with the highest on Day 7 and

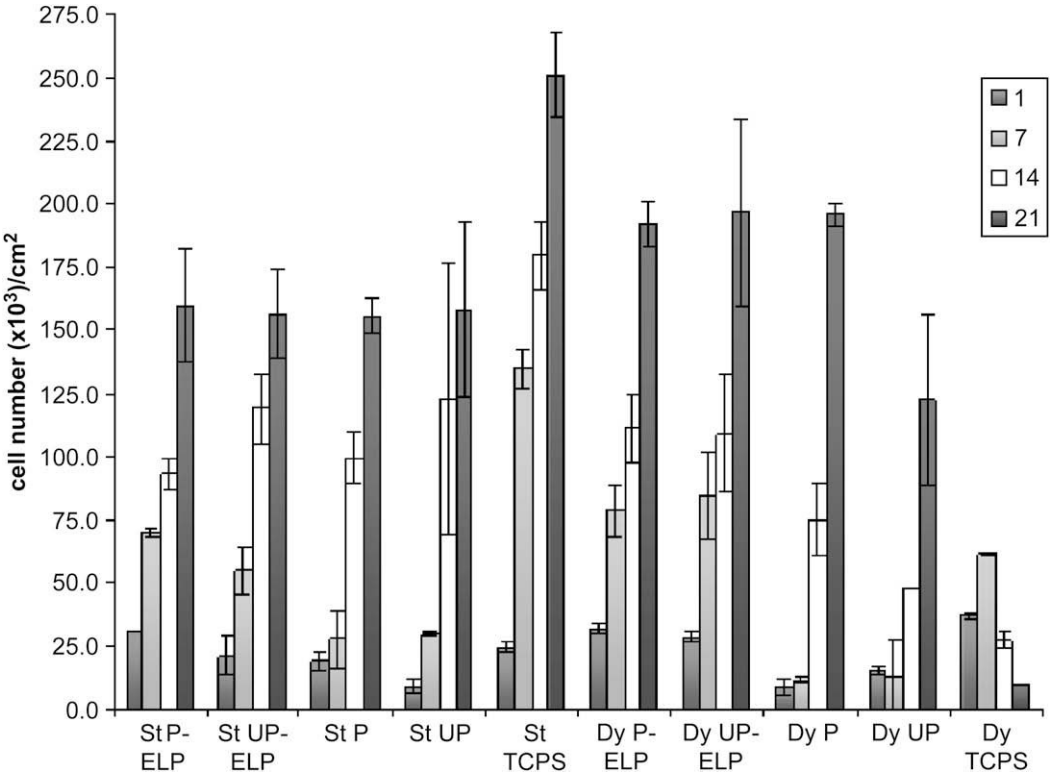

Fig. 5. Cell proliferation on the pNIPAM films with different surface topography and chemistry under static and dynamic conditions, and on TCPS for upto 21 days (St: static, Dy: dynamic, P: patterned, UP: unpatterned, ELP: ELP adsorbed).

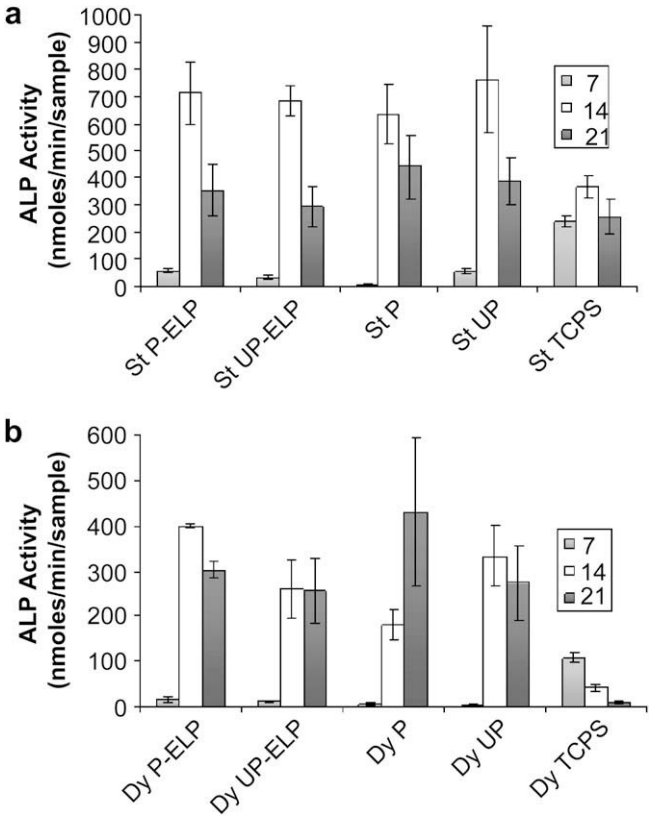

Fig. 6. ALP activity on TCPS and on the polymeric films with different topography and surface chemistry cultured under (a) static and (b) dynamic conditions for upto 21 days (St: static, Dy: dynamic, P: patterned, UP: unpatterned, ELP: ELP adsorbed).

the lowest on Day 21 (Fig. 7a and b). However, the St TCPS and Dy TCPS specific ALP activities were close to each other. Specific ALP activities obtained for the static group were much higher than their counterparts in the dynamic group on Day 7. There were two factors which could explain relatively low values of specific ALP activities obtained with the dynamic group; (1) decrease of temperature for short periods (29 ^{o}C, 15 min) and, (2) tensile stress applied to the cells by the pNIPAM films during the temperature cycle. On the other hand the control groups (Dy TCPS) did not receive any mechanical stress from the system and they were only exposed to cyclic temperature decreases. The similarity of specific ALP activities on St TCPS, which were incubated at 37 ^{o}C throughout the test, and Dy TCPS suggests that temperature decrease has no noticeable effect on the ALP activities of cells. Therefore, it can be stated that the relative decrease in specific ALP activity observed in the dynamic group when compared to the static group was because of the tensile stress generated by the pNIPAM films under the defined conditions (cyclic temperature changes).

In the second week, when cells were no longer cultured under dynamic conditions (the cyclic loading was applied between days 2 and 6), increases in the specific ALP activities were observed for all groups, except Dy TCPS. The relative increase in the specific ALP activities during the second week for the Dy P-ELP, Dy UP-ELP and Dy UP were much higher than their counterparts in the static group, but still were not comparable. This interesting finding might suggest that the ability of pNIPAM films to deliver mechanical stress differs when they are patterned and unpatterned, but it is not enough to explain the low specific ALP activity on Dy UP-ELP. It was shown that ELP played a role in cell attachment leading to better cell–material interaction and retained the cells in attached form on the surface under dynamic conditions. Therefore, it can be stated that ELP adsorption enhanced the cell–material communication and thus cells seeded on ELP coated surfaces were subject to higher

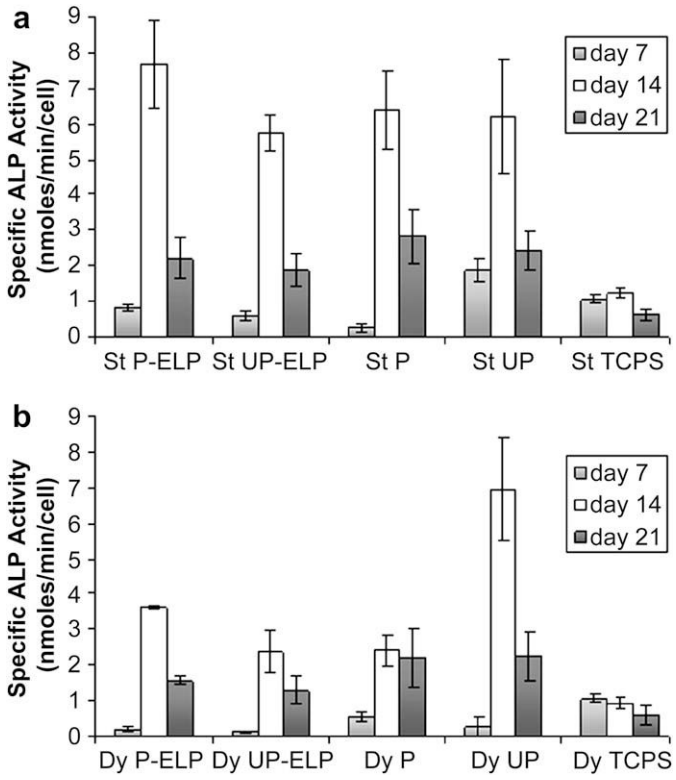

Fig. 7. Specific ALP activity on TCPS and on the polymeric films with different topography and surface chemistry under (a) static and (b) dynamic conditions.

mechanical stress. On the other hand, when there was no ELP on the surface, the cell–material interaction was not as good because of the formation of a hydration layer between the cells and pNIPAM when the temperature was decreased, but despite this disadvantage, patterns on the surface of pNIPAM might have increased the cell–material interaction by retaining the cells in the grooves. Also the patterns on the films seemed to affect specific ALP activity positively both under static and dynamic conditions when ELP is present, (Fig. 7a and b). The differences in specific ALP activities between St P-ELP and St UP-ELP in the static group and Dy P-ELP and Dy UP-ELP in the dynamic group were significant. In the absence of ELP, however, patterns did not seem to affect specific ALP activity in the static group, in which there was no weakened cell attachment and so no differences could be seen between the ELP adsorbed and unadsorbed films in terms of cell attachment as in dynamic group. ELP adsorbed patterned films had slightly higher specific ALP activity values than ELP-free patterned films in the static group and significantly higher in the dynamic group. When unpatterned ELP adsorbed and ELP-free static films (St UP-ELP and St UP) were compared, however, there was almost no difference. So, it can be concluded that neither ELP nor patterns alone have a direct effect on the specific ALP activity, but together, they have a positive influence.

3.3.3. *Fluorescence microscopy*

Fluorescence micrographs of 21 day static cultured cells were obtained. Nuclear staining with DAPI showed that the cell nuclei (blue) were aligned parallel to each other on the patterned films and seemed to elongate along the axis (Fig. 8a, c and d), whereas random cell orientation occurred on unpatterned films (Fig. 8b and e). FITC-labelled Phalloidin staining also showed that the cell cytoskeletons (green) were oriented in the direction of the axis meaning the cell guidance by physical topography was achieved (Fig. 8c and d). Fig. 8e shows cells on the unpatterned, ELP adsorbed film where curved actin bundles unlike those on the patterned films are seen.

3.3.4. *SEM*

Scanning electron micrographs of cells cultured under static and dynamic conditions on patterned and unpatterned pNIPAM films were obtained at the end of 2 and 3 weeks incubation. At the end of the second week, cell sheets were observed on the patterned films (Fig. 9). The cells were found to be attached on the side-walls of the grooves or within the grooves and also stretched between the walls perpendicular to the axis. Day 21 micrographs of samples were similar to those of Day 14 in terms of cell attachment (figures not shown). Cells were found within the grooves and stretched between the ridges.

3.3.5. *Mineralization*

To detect mineralization, the films were stained with tetracycline and examined with fluorescence microscopy at 480 nm. Mineralization was observed on all the films (figures not shown). This finding, along with the ALP activity results suggests that pNIPAM can be considered as a good scaffold material for enhanced osteogenic differentiation. XPS applied with SEM showed presence of calcium and phosphate on all of the cell seeded samples. The molar ratio of calcium to phosphate was found to be 1.56 ± 0.21, which is close but lower than that of the calcium to phosphate ratio of bone hydroxyapatite (1.67).

4. Discussion

Stimuli-responsive (smart) polymers have potential for use in a wide variety of applications in biotechnology. In this study, pNIPAM films were prepared to serve as intelligent cell carriers which can respond to temperature changes and apply mechanical stress on cells seeded onto them to induce bone formation. Micropatterns were formed on the surface of the polymers by using silicon wafers and the film surfaces were further chemically modified by ELP adsorption to promote cell adhesion with RGD amino acid sequences.

Swelling studies showed that the pNIPAM films had an LCST in the same range as those found in the literature (w32 ^{o}C). Dynamic culturing temperatures were chosen as 29 and 37 ^{o}C, which are below and above the LCST, respectively, to induce hydrophilic/hydrophobic changes in the polymer resulting in dimension changes of the film. The mechanical strain that could be created was found to vary around 6%, which is significantly higher than the range observed with physiologically loaded bone.

ELP adsorbed surfaces had more cells on the first day of static culture, which shows that the ELP adsorption enhanced cell attachment. The importance of the cell attachment sequences in ELP became more apparent when the cells were cultured under dynamic conditions. It was found that the increased hydrophilicity at 29 ^{o}C resulted in a decrease of cell number; comparable cell numbers were found on ELP adsorbed films in the dynamic and the static groups. However, when the cyclic processes were stopped, ELP-free films of the dynamic group reached comparable cell numbers with all the films in the static group. This finding showed that ELP adsorption enhanced initial cell attachment, but this was effective only in the initial stages. For the dynamic culture of the cells where temperature decrease was used, ELP was more crucial in retaining the cells in attached state. A significant decrease in cell number was observed on dynamic TCPS in which cells were subjected to temperature changes but could not receive the benefits of the mechanical stress because TCPS did not respond to temperature changes. On the other hand, the cells grown in

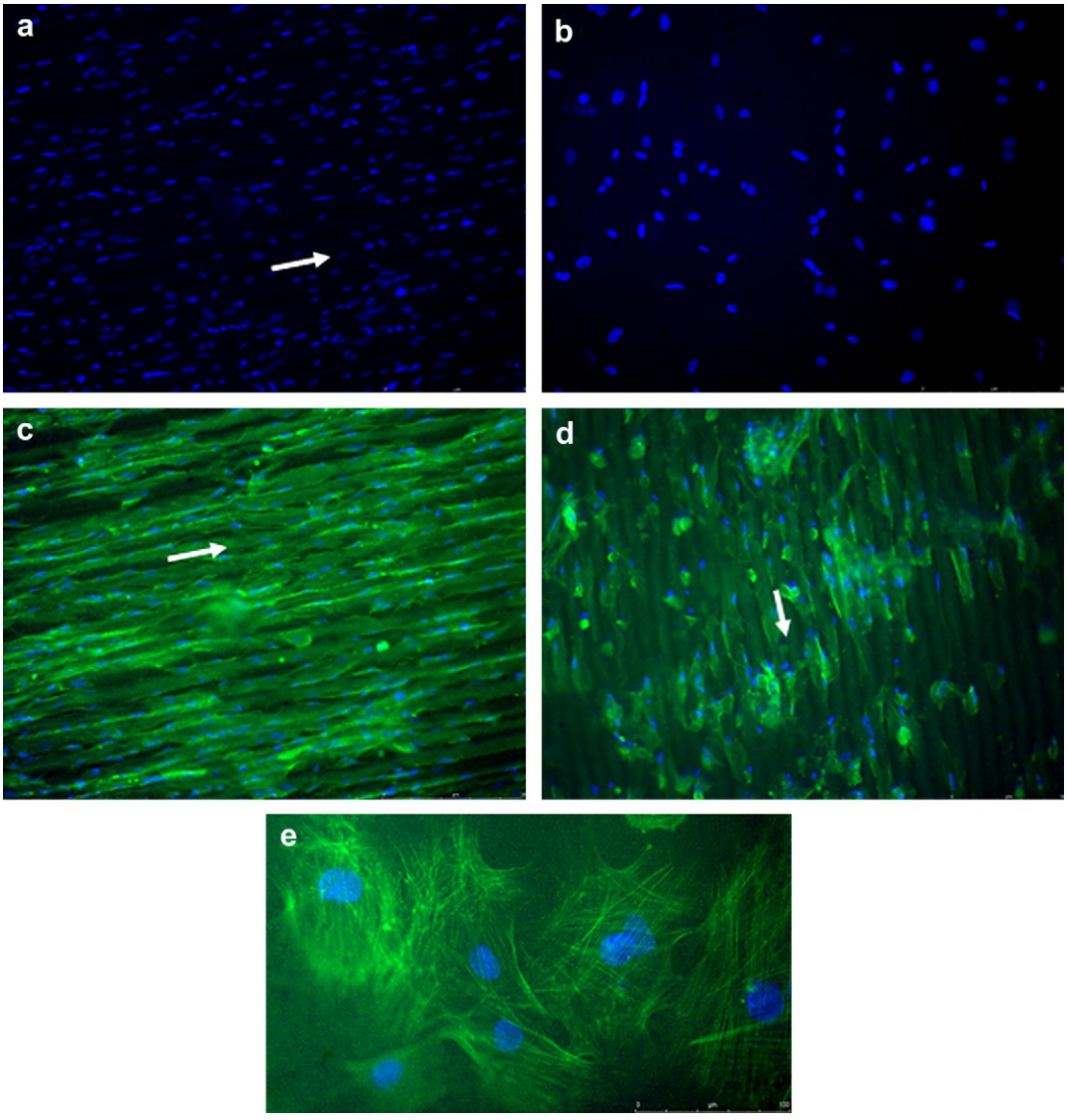

Fig. 8. Fluorescence micrographs of (a) DAPI stained P-ELP film (x10), (b) DAPI stained UP-ELP film (x10), (c) double stained (DAPI and Phalloidin) P-ELP film (x10), (d) P film (x10), and (e) UP-ELP film (x20). Directions of the pattern axis are as shown by the arrows.

dynamic culture showed an increase in number similar to the static group. This finding suggested that increased proliferation was a result of mechanical stress. There are many studies that report increased osteoblast proliferation in response to mechanical stress [28–35] and only a few that report a decrease [36,37]. These controversial results may arise from the different magnitudes and frequencies of stress applied [38]. The method used in this study- using temperature changes- to load mechanical stress onto the cells is unique, and therefore, any comparison from the literature is difficult.

Specific ALP activity was used as a differentiation marker. They were the highest on Day 14. Mechanical strain introduced to the cells in the dynamic group was found to decrease the specific ALP activity when compared with the static group. Similar results have been reported by other groups working on effect of mechanical stress on osteoblast differentiation. Chen et al. applied strain mechanically to the level of 3% or 10% by surface elongation at 1 Hz for 8 or 48 h on human mesenchymal stem cells [39]. They also added another experimental group which included cells that rested for 48 h after the end of the mechanical stretching for 48 h to explore if the effects of mechanical stretching were transient. They found that 3% stretching induced upregulation of ALP gene expression at 8 h significantly but downregulation at 48 h and the value returned to the basal level of the unstretched control after the stretched cells had rested for 48 h. In the 10% stretched groups, the ALP mRNA level did not change significantly at 8 or 48 h but down regulated when the cells were left to relax for 48 h. In another study, Koike et al. used the bone marrow stromal cell line ST2 to investigate osteoblastic differentiation under 0.8%, 5%, 10%, and 15% elongation at 1 Hz for 2 days [30]. They found that ALP activities of cells stretched by 0.8% and 5% significantly increased at 24 h but no significant change in ALP activity was observed in the 5% elongation group at 48 h. As observed in the current study, ALP activities of the 10% and 15% elongation groups significantly decreased. Similarly Yamaguchi et al. reported that the ALP activity in periodontal ligament (PDL) cells obtained from a 12 year old male patient decreased by 10–42% upon application of a tensile force to increase the surface area by 9–24% [40]. The deformation of cells was found to be above the physiologic conditions (5.9% ± 2.3%) in this study, it was, therefore, concluded that the system applied high magnitude

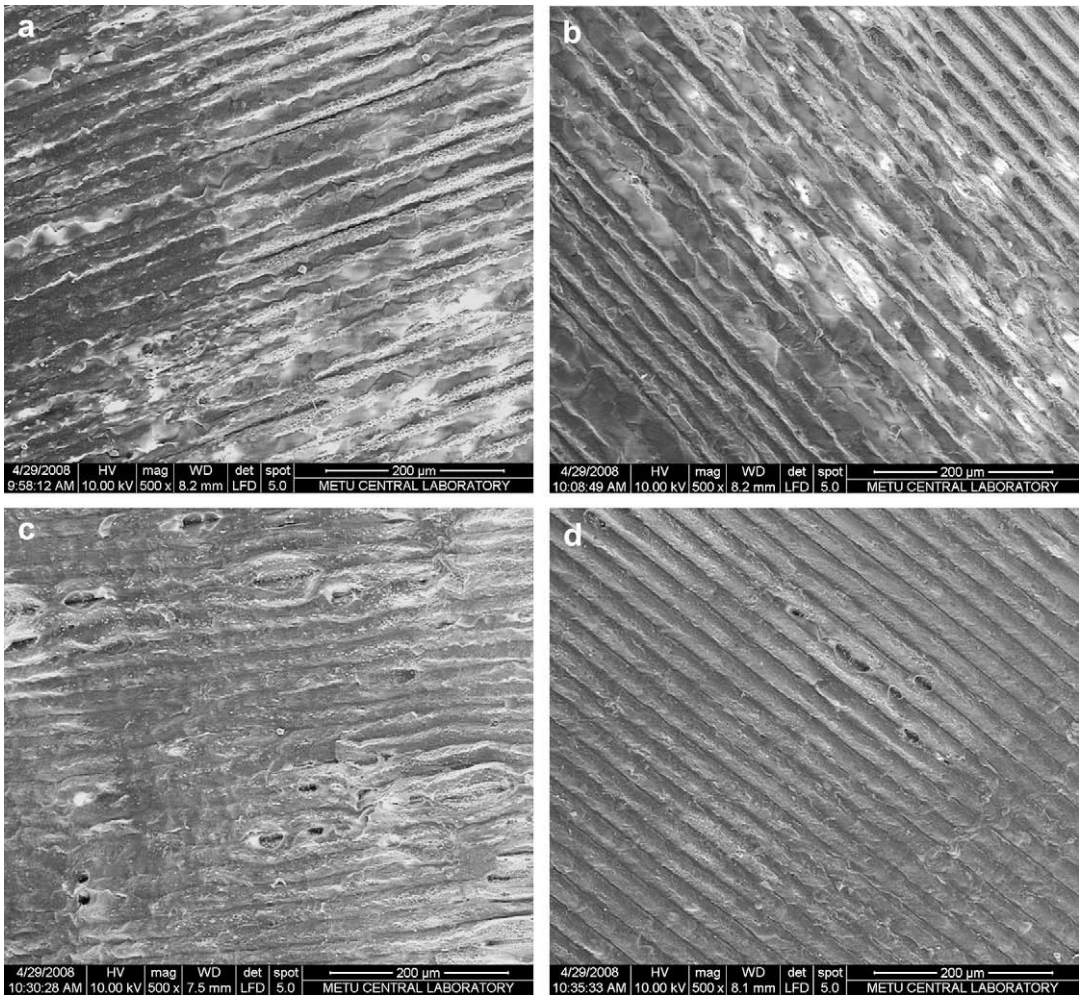

Fig. 9. SEM micrographs of patterned films on Day 1\of culture. (a) St P-ELP, (b) St P, (c) Dy P-ELP, (d) Dy P. Magnification: x500.

mechanical stress to the cells. There are contradictory reports in the literature about the influence of strain on ALP activity. According to one [37], a strain higher than in this study (12%) did not alter the ALP activity, but others lower than 1.8% strain showed that ALP activity was increased [29,32,33,41] or decreased [31] with strain. The different results obtained from these studies might be dependent on the frequency and the type of the mechanical stress (intermittent, continuous), the type of the cells and the *in vitro* conditions as well as time and the length of the mechanical stress application.

Interestingly, Dy UP, a film free of patterns and ELP, showed comparable specific ALP activity to the others in the static group. This finding suggested that the ability of pNIPAM films to transfer the mechanical stress on the cells differs even when they are unpatterned. ELP adsorption was shown to play an important role in the transfer of mechanical stress by enhancing the cell–material interaction based on the decreased specific ALP activity on Dy UP-ELP films similar to Dy P-ELP films.

The specific ALP results obtained with all the pNIPAM films, both static and dynamic, were higher than those obtained with TCPS on Days 14 and 21. Therefore, it can be stated that pNIPAM films used in this study support the differentiation of BMSC more than TCPS. Similarly Smith et al. found that multipotent C2C12 cells exhibited ALP activity on RGD grafted p(NIPAM/NASI) surfaces significantly higher than those on TCPS under static conditions [42]. Unlike in the present study, where ELP was adsorbed on patterned pNIPAM surfaces, they did not observe a specific effect of RGD grafting on ALP activity of cells, and concluded that p(NIPAM/NASI) surfaces were more conducive for the expression of ALP.

5. Conclusion

ELP has proven itself as a cell adhesion promoter, a property critical for tissue engineering. pNIPAM films were shown to be promising cell carriers for tissue engineering purposes and to study the effect of mechanical stress on cells which can compete with the mechanical processes designed to apply mechanical stress. Thus, the ELP-pNIPAM combination is a very good model to study tissue engineering and the influence of mechanical stress. One disadvantage of the current system may be the non-degradability of pNIPAM which does not make it suitable for implantation into the body but it is possible to make pNIPAM degradable by adding hydrolysable groups to overcome this situation. Another approach also considered in this study could be using pNIPAM as a substrate and covering it with a biodegradable biomaterial that cells would like to interact and just before the implantation removing pNIPAM and transferring the cells and the underlying biomaterial to the body. Depending on the cell–cell interaction strength a cell sheet might be lifted off the surface by changing the temperature to be implanted.

Acknowledgements

This study was supported by a grant from METU Graduate School of Natural and Applied Sciences (BAP-2006-07-02-00-01), EU FP6 project BioPolySurf, MICINN (projects MAT 2007-66275-C02-01 and NAN2004-08538), the JCyL (projects VA087A06, VA030/08 and VA030A08), the Ciber-BBN (project CB06-01-0003), and the JCyL and the Instituto de Salud Carlos III under the ''Network Center of Regenerative medicine and Cellular Therapy of Castilla and León''and a scholarship to N.O. by the State Planning Organization (BAP 08-01-DPT2003K.120920-20).

Appendix

Figures with essential colour discrimination. Certain figures in this article, in particular Fig. 8, are difficult to interpret in black and white. The full colour images can be found in the on-line version, at doi:10.1016/j.biomaterials.2009.06.044.

References

[1] Rotter N, Haisch A, Bucheler M. Cartilage and bone tissue engineering for reconstructive head and neck surgery. Eur Arch Otorhinolaryngol 2005;262:539–45.
[2] Laurencin CT, Ambrosio AMA, Borden MD, Cooper Jr JA. Tissue engineering: orthopedic applications. Annu Rev Biomed Eng 1999;1:19–46.
[3] Burg KJL, Porter S, Kellam JF. Biomaterial developments for bone tissue engineering. Biomaterials 2000;21:2347–59.
[4] Rose FRAJ, Oreffo ROC. Bone tissue engineering: hope vs. hype. Biochem Biophys Res Commun 2002;292:1–7.
[5] Brandl F, Sommer F, Goepferich A. Rational design of hydrogels for tissue engineering: impact of physical factors on cell behavior. Biomaterials 2007;28:134–46.
[6] Liu WF, Chen CS. Engineering biomaterials to control cell function. Mater Today 2005;8:28–35.
[7] Rodríguez-Cabello JC, Reguera J, Girotti A, Alonso M, Testera AM. Developing functionality in elastin-like polymers by increasing their molecular complexity: the power of the genetic engineering approach. Prog Polym Sci 2005;30:1119–45.
[8] Arias FJ, Reboto V, Martín S, López I, Rodríguez-Cabello JC. Tailored recombinant elastin-like polymers for advanced biomedical and nano(bio)technological applications. Biotechnol Lett 2006;28:687–95.
[9] Rodríguez-Cabello JC, Prieto S, Reguera J, Arias FJ, Ribeiro A. Biofunctional design of elastin-like polymers for advanced applications in nano-biotechnology. J Biomater Sci Polym Ed 2007;18:269–86.
[10] Urry DW. What sustains life? Consilient mechanisms for protein-based machines and materials. New York: Springer-Verlag; 2006. 488–540.
[11] Meyer DE, Trabbic-Carlson K, Chilkoti A. Protein purification by fusion with an environmentally responsive elastin-like polypeptide: effect of polypeptide length on the purification of thioredoxin. Biotechnol Prog 2001;17:720–8.
[12] Meyer DE, Kong GA, Dewhirst MW, Zalutsky MR, Chilkoti A. Targeting a genetically engineered elastin-like polypeptide to solid tumors by local hyperthermia. Cancer Res 2001;61:1548–54.
[13] Herrero-Vanrell R, Rincón AC, Alonso M, Reboto V, Molina-Martinez IT, Rodríguez-Cabello JC. Self-assembled particles of an elastin-like polymer as vehicles for controlled drug release. J Control Release 2005;102:113–22.
[14] Girotti A, Reguera J, Rodríguez-Cabello JC, Arias FJ, Alonso M, Testera AM. Design and bioproduction of a recombinant multi(bio)functional elastin-like protein polymer containing cell adhesion sequences for tissue engineering purposes. J Mater Sci Mater Med 2004;15:479–84.
[15] Liu JC, Tirrell DA. Cell response to RGD density in cross-linked artificial extracellular matrix protein films. Biomacromolecules 2008;9:2984–8.
[16] Mullender M, El Haj AJ, Yang Y, van Duin MA, Burger EH, Klein-Nulend J. Mechanotransduction of bone cells in vitro: mechanobiology of bone tissue. Med Biol Eng Comput 2004;42:14–21.
[17] Vico L, Collet P, Guignandon A, Lafage-Proust MH, Thomas T, Rehailia M, et al. Effects of long-term microgravity exposure on cancellous and cortical weight-bearing bones of cosmonauts. Lancet 2000;355:1607–11.
[18] Leblanc AD, Schneider VS, Evans HJ, Engelbretson DA, Krebs JM. Bone mineral loss and recovery after 17 weeks of bed rest. J Bone Miner Res 1990;5:843–50.
[19] Simkin A, Ayalon J, Leichter I. Increased trabecular bone density due to bone-loading exercises in postmenopausal osteoporotic women. Calcif Tissue Int 1987;40:59–63.
[20] Leclerc E, David B, Griscom L, Lepioufle B, Fujii T, Layrolle P, et al. Study of osteoblastic cells in a microfluidic environment. Biomaterials 2006;27: 586–95.
[21] Meyer U, Buchter A, Nazer N, Wiesmann HP. Design and performance of a bioreactor system for mechanically promoted three-dimensional tissue engineering. Br J Oral Maxillofac Surg 2006;44:134–40.
[22] Li J, Chen G, Zheng L, Luo S, Zhao Z. Osteoblast cytoskeletal modulation in response to compressive stress at physiological levels. Mol Cell Biochem 2007;304:45–52.
[23] Walboomers XF, Elder SE, Bumgardner JD, Jansen JA. Hydrodynamic compression of young and adult rat osteoblast-like cells on titanium fiber mesh. J Biomed Mater Res A 2006;76:16–24.
[24] Di Palma F, Douet M, Boachon C, Guignandon A, Peyroche S, Forest B, et al. Physiological strains induce differentiation in human osteoblasts cultured on orthopaedic biomaterial. Biomaterials 2003;24:3139–51.
[25] de las Heras Alarcon C, Pennadam S, Alexander C. Stimuli responsive polymers for biomedical applications. Chem Soc Rev 2005;34:276–85.
[26] Kenar H, Kocabas A, Aydinli A, Hasirci V. Chemical and topographical modification of PHBV surface to promote osteoblast alignment and confinement. J Biomed Mater Res A 2008;85:1001–10.
[27] Matsuzaka K, Walboomers XF, de Ruijter JE, Jansen JA. The effect of poly-L-lactic acid with parallel surface micro groove on osteoblast-like cells in vitro. Biomaterials 1999;20:1293–301.
[28] Ignatius A, Blessing H, Liedert A, Schmidt C, Neidlinger-Wilke C, Kaspar D, et al. Tissue engineering of bone: effects of mechanical strain on osteoblastic cells in type I collagen matrices. Biomaterials 2005;26:311–8.
[29] Ushida T, Uemura T, Tateishi T. Changes in cell proliferation, alkaline phosphatase activity and cAMP production by mechanical strain in osteoblast-like cells differentiated from rat bone marrow. Mater Sci Eng C 2001;17:51–3.
[30] Koike M, Shimokawa H, Kanno Z, Ohya K, Soma K. Effects of mechanical strain on proliferation and differentiation of bone marrow stromal cell line ST2. J Bone Miner Metab 2005;23:219–25.
[31] Winter LC, Walboomers XF, Bumgardner JD, Jansen JA. Intermittent versus continuous stretching effects on osteoblast-like cells in vitro. J Biomed Mater Res A 2003;67:1269–75.
[32] Jackson RA, Kumarasuriyar A, Nurcombe V, Cool SM. Long-term loading inhibits ERK1/2 phosphorylation and increases FGFR3 expression in MC3T3-E1 osteoblast cells. J Cell Physiol 2006;209:894–904.
[33] Qi MC, Hu J, Zou SJ, Chen HQ, Zhou HX, Han LC. Mechanical strain induces osteogenic differentiation: Cbfa1 and Ets-1 expression in stretched rat mesenchymal stem cells. Int J Oral Maxillofac Surg 2008;37:453–8.
[34] Tang LL, Xian CY, Wang YL. The MGF expression of osteoblasts in response to mechanical overload. Arch Oral Biol 2006;51:1080–5.
[35] Fermor B, Gundle R, Evans M, Emerton M, Pocock A, Murray D. Primary human osteoblast proliferation and prostaglandin E2 release in response to mechanical strain in vitro. Bone 1998;22:637–43.
[36] Labat B, Chepda T, Frey J, Rieu J, Aurelle JL, Douet M, et al. Practice of a testing bench to study the effects of cyclic stretching on osteoblast-orthopaedic ceramic interactions. Biomaterials 2000;21:1275–81.
[37] Singh SP, Chang EI, Gossain AK, Mehara BJ, Galiano RD, Jensen J, et al. Cyclic mechanical strain increases production of regulators of bone healing in cultured murine osteoblasts. J Am Coll Surg 2007;204:426–34.
[38] Kaspar D, Seidl W, Neidlinger-Wilke C, Beck A, Claes L, Ignatius A. Proliferation of human-derived osteoblast-like cells depends on the cycle number and frequency of uniaxial strain. J Biomech 2002;35:873–80.
[39] Chen YJ, Huang CH, Lee IC, Lee YT, Chen MH, Young TH. Effects of cyclic mechanical stretching on the mRNA expression of tendon/ligament-related and osteoblast-specific genes in human mesenchymal stem cells. Connect Tissue Res 2008;49:7–14.
[40] Yamaguchi M, Shimizu N, Shibata Y, Abiko Y. Effects of different magnitudes of tension-force on alkaline phosphatase activity in periodontal ligament cells. J Dent Res 1996;75:889–94.
[41] Di Palma F, Guignandon A, Chamson A, Lafage-Proust MH, Laroche N, Peyroche S, et al. Modulation of the responses of human osteoblast-like cells to physiologic mechanical strains by biomaterial surfaces. Biomaterials 2005;26:4249–57.
[42] Smith E, Yang J, McGann L, Sebald W, Uludag H. RGD-grafted thermoreversible polymers to facilitate attachment of BMP-2 responsive C2C12 cells. Biomaterials 2005;26:7329–38.